medRxiv preprint doi: https://doi.org/10.64898/2026.08.18.26360688; this version posted August 21, 2026. The copyright holder for this preprint (which was not certified by peer review) is the author/funder, who has granted medRxiv a license to display the preprint in perpetuity. It is made available under a CC-BY-NC-ND 4.0 International license .

Metagenomic Sequencing for Wastewater-Based Surveillance: Modeling and Experimental Approaches for Determining Limit of Detection

Amy Xiao[1], Katherine Besse[1], Daisy Connors[1], Trina Vian[1], Jim Stylinski[1], Anthony Mannion[1], Joe Lacirignola[1]*

1. Lincoln Laboratory, Massachusetts Institute of Technology, Lexington, MA, USA

* Corresponding author

Contributions

AX Data Curation, Formal Analysis, Investigation, Software, Visualization, Writing

KB Data Curation, Investigation, Writing

DC Data Curation, Investigation, Writing

TV Conceptualization, Investigation, Visualization, Writing

JS Data Curation, Formal Analysis, Investigation, Software, Visualization

AM Data Curation, Formal Analysis, Software, Visualization, Writing

JL Conceptualization, Investigation, Visualization, Writing

DISTRIBUTION STATEMENT A. Approved for public release. Distribution is unlimited.

This material is based upon work supported by the Under Secretary of War for Research and Engineering under Air Force Contract No. FA8702-15-D-0001 or FA8702-25-D-B002. Any opinions, findings, conclusions or recommendations expressed in this material are those of the author(s) and do not necessarily reflect the views of the Under Secretary of War for Research and Engineering.© 2026 Massachusetts Institute of Technology.

Delivered to the U.S. Government with Unlimited Rights, as defined in DFARS Part 252.227-7013 or 7014 (Feb 2014). Notwithstanding any copyright notice, U.S. Government rights in this work are defined by DFARS 252.227-7013 or DFARS 252.227-7014 as detailed above. Use of this work other than as specifically authorized by the U.S. Government may violate any copyrights that exist in this work.

NOTE: This preprint reports new research that has not been certified by peer review and should not be used to guide clinical practice.

medRxiv preprint doi: https://doi.org/10.64898/2026.08.18.26360688; this version posted August 21, 2026. The copyright holder for this preprint (which was not certified by peer review) is the author/funder, who has granted medRxiv a license to display the preprint in perpetuity. It is made available under a CC-BY-NC-ND 4.0 International license .

ABSTRACT

Since the COVID-19 pandemic, wastewater-based surveillance (WBS) has emerged as a key approach to assess community-level health and the evolution of pathogens. To date, most established WBS systems focus on polymerase chain reaction (PCR) based detection and targeted sequencing of known pathogens because these approaches are well-accepted and include amplification of pathogen target sequences of interest thereby enabling lower limits of detection. Metagenomic next-generation sequencing (mNGS) is a promising approach to enable pathogen detection and surveillance beyond predefined pathogen lists, but its regular application to WBS has not been yet widely adopted because many key performance characteristics are not well-understood, including limit of detection (LOD) and false positive/negative rates. This paper describes a computational analysis to estimate the operational LOD of various sequencing approaches using a simplified model of a local wastewater (WW) system involving a military base. This paper also presents findings from two types of experiments: 1) laboratory-spiked, those for which *Atlantibacter subterraneus* (Asub) is introduced into real-world WW samples in a laboratory setting, and 2) system-spiked, those for which Asub is introduced at a source location of a real-world WW system. Findings indicate that mNGS detection performance varies with sequencing method and the data analysis process. In addition, findings indicate that site-specific method characterization should be used when implementing mNGS for WBS because sites can have different WW system configurations, background organisms and sequencing inhibitors.

INTRODUCTION

Widely implemented during the COVID-19 pandemic, wastewater-based surveillance (WBS) enables community-level disease monitoring and provides an early warning of pathogen spread and evolution. Many groups have shown that SARS-CoV-2 detections in wastewater preceded widespread clinical reporting. [1,2,3,4,5] It has been previously demonstrated that SARS-CoV-2 viral copy numbers in wastewater were higher than expected from confirmed clinical cases,[6,7,8,9,10] suggesting that WBS may form

medRxiv preprint doi: https://doi.org/10.64898/2026.08.18.26360688; this version posted August 21, 2026. The copyright holder for this preprint (which was not certified by peer review) is the author/funder, who has granted medRxiv a license to display the preprint in perpetuity. It is made available under a CC-BY-NC-ND 4.0 International license .

a more comprehensive picture of community health and could provide early warning of outbreaks, due to the contribution of asymptomatic shedders or those who do not seek clinical care. Currently, public health agencies, including the United States Centers for Disease Control and Prevention (CDC), use quantitative polymerase chain reaction (qPCR) and targeted sequencing to monitor for the presence of a pre-determined list of pathogens.[11] Both qPCR-based and targeted sequencing methods enable the tracking of temporal trends in pathogen levels via longitudinal analysis.[12,13]

While targeted methods have been routinely used to provide public health information, the COVID-19 pandemic demonstrates the challenges that a rapidly evolving pathogen poses for PCR-based detection methods. Furthermore, there is an ever-growing risk of novel and emerging pathogens due to human encroachment of natural habitats, climate change, rapid global travel and increasing use of artificial intelligence and access to biotechnology[14,15,16] These risk factors underscore the need to detect potential pathogens in a sample without prior pathogen knowledge. For this effort, we focus on metagenomic next generation sequencing (mNGS) (or 'shotgun' sequencing) as the technical approach to broadly characterize the nucleic acid present in WW samples for organism identification.

mNGS can been used to characterize the microbial composition of a sample, enabling extensive human and environmental microbiome studies.[17,18,19,20,21,22,23,24] However, the operational use of mNGS (i.e., serving as a basis for public health decision making, development of infectious disease diagnostics, and environmental biological pathogen detection[25,26,27]) has been hindered by several challenges, including complex non-standardized workflows, lack of understanding of detection metrics such as the limit of detection (LOD), difficulty relating pathogen sequencing reads to the associated disease risks and the overall cost per sample analysis. As a result, there are currently no FDA-approved mNGS diagnostic tests,[28] and mNGS approaches have not been widely adopted for operational wastewater surveillance.

Several recent journal articles have provided insights into LOD and other mNGS performance metrics.[29, 30,31,32,33,] The studies typically vary in terms of the workflow, sequencing type and depth, what is used to generate a gold standard result, and how detection metrics are calculated. As a result, it is difficult

medRxiv preprint doi: https://doi.org/10.64898/2026.08.18.26360688; this version posted August 21, 2026. The copyright holder for this preprint (which was not certified by peer review) is the author/funder, who has granted medRxiv a license to display the preprint in perpetuity. It is made available under a CC-BY-NC-ND 4.0 International license .

to compare results across different efforts. To understand the potential advantage of mNGS-based wastewater surveillance approaches, both modeling and experimental approaches are necessary to assess feasibility and actionability. To this end, Grimm et al. used statistical modelling approaches to quantify the sensitivity and cost of mNGS-based wastewater surveillance for viral pathogen detection, finding that relative abundance of SARS-CoV-2 varied by orders of magnitude across studies and that hybridization panels can greatly reduce cost and improve sensitivity.[34] A pilot study on the implementation of wastewater surveillance at skilled-nursing facilities conducted dye-based tracer studies to assess feasibility of additional sites.[35] Sonnenwald et al. conducted fluorescent dye tracing at the sewer network level and developed a simplified hydraulic modeling approach to predict solute concentrations across the network following an injection of dye.[36] Kohle et al. flushed 10^{13} CFU of *Staphylococcus hyicus* in a sewershed of ~36,000 people and showed a sensitivity of 16-140 sick people based on shotgun metagenomic sequencing from samples collected at the wastewater treatment plant.[37] These studies emphasize the importance of characterizing performance metrics like sensitivity and limit of detection to demonstrate the utility of shotgun metagenomic sequencing for WBS-informed public health decisions.

In this study, we explore methods to characterize the operational LOD for wastewater mNGS and various sampling architectures using both theoretical and experimentally-derived results. We define the operational LOD as the lowest concentration of an analyte that can be reliably distinguished from a blank sample in the operationally-relevant context (here, a wastewater system). To assess the theoretical performance of mNGS, inform field experiments and derive cost estimates, we built a computational model of a local wastewater system network to estimate the performance of qPCR and mNGS to enable the potential detection of a range of pathogen-infected cases shedding into the wastewater system of a military base. The computational analysis was conducted for a set of individual cases (as well as higher levels of cases) shedding into the wastewater system. This paper presents the performance estimates for the detection of a single case, as this is the most stressing scenario and one that could potentially enable the earliest detection of an emerging novel pathogen. To validate model findings, we conducted a laboratory-based

medRxiv preprint doi: https://doi.org/10.64898/2026.08.18.26360688; this version posted August 21, 2026. The copyright holder for this preprint (which was not certified by peer review) is the author/funder, who has granted medRxiv a license to display the preprint in perpetuity. It is made available under a CC-BY-NC-ND 4.0 International license .

spike test to assess the feasibility of detection with untargeted metagenomic sequencing in wastewater. We then conducted wastewater system-spike experiments to measure the operational mNGS LOD for a local wastewater system for different sequencing technologies and analysis methods. Collectively, the combination of computational and laboratory insights and validation through experimental results provides a method for defining mNGS performance for wastewater systems.

MATERIALS AND METHODS

Computational model development and assumptions:

To inform LOD organism-spike experiments, an estimate of genomic target concentration and dwell time as a function of sampling location was needed to guide study design. A WW network model was developed and configured to emulate Hanscom Air Force Base (HAFB) where system spike experiments would be performed. HAFB consists of multiple building types including varying types of commercial and residential structures. The complex base WW network was simplified to reduce computational complexity and time. Simplifying assumptions to reduce complexity included neglecting stormwater runoff and infiltration, combining adjacent commercial or residential areas as a single source where practical and defining "system manholes" (i.e., discrete sampling points within the model) at main sewage line junctions. Finer sampling resolution was retained within the MIT Lincoln Laboratory complex to support follow-on experimentation. A schematic of the simplified network is shown in Figure S1**.** Pipe material type, diameter and approximate run length were identified directly from specifications provided by HAFB personnel.

In the simplified model, a 1D advection and dispersion equation was coupled with series routing logic and exponential decay of target concentration over time. The modeling of advection and dispersion of solutes within a fluid is given by the equation:

$$\frac{\partial c}{\partial t} + U\frac{\partial c}{\partial x} = D\frac{\partial^2 c}{\partial x^2} \quad (1)$$

medRxiv preprint doi: https://doi.org/10.64898/2026.08.18.26360688; this version posted August 21, 2026. The copyright holder for this preprint (which was not certified by peer review) is the author/funder, who has granted medRxiv a license to display the preprint in perpetuity. It is made available under a CC-BY-NC-ND 4.0 International license .

where c = concentration (gene-copies/mL), U = velocity (m/s), D = dispersion coefficient. The concentration with respect to distance along x and time, *t,* is:

$$c(x_2, t) = \int_{-\infty}^{\infty} \frac{Uc(x_1, \gamma)}{\sqrt{4\pi D\bar{t}}} exp\left(-\frac{U^2(\bar{t} - t + \gamma)^2}{4D\bar{t}}\right) d\gamma \quad (2)$$

To model the degradation of RNA with time in WW, the SARS-CoV-2 virus was selected as a representative pathogen due to extensive WW characterization that occurred during the COVID-19 pandemic. The concentration of SARS-CoV-2 RNA is modeled using [38].

$$c(t) = c(0)e^{-kt} \quad (3)$$

Additional simplifying assumptions (related to solute transport and degradation) include: steady-state gravity flow within pipes, pressure main between wet-well pump stations is treated as time delay, longitudinal dispersion is characterized by the Manning equation [39],

$$Q = \frac{1.49}{\eta} AR^{2/3}S^{1/2} \quad (4)$$

where Q = discharge,

η = Manning's roughness coefficient,

A = area,

R= hydraulic radius,

S= slope.

target organism is injected into the system at the beginning of a simulation, lower station pump runs continuously, and sampling performed at any point in the network is lossless. Other model parameters are listed in Table 1. Water usage estimates were obtained from the Massachusetts state environmental code for establishment type[40] and summarized in Table S1.

medRxiv preprint doi: https://doi.org/10.64898/2026.08.18.26360688; this version posted August 21, 2026. The copyright holder for this preprint (which was not certified by peer review) is the author/funder, who has granted medRxiv a license to display the preprint in perpetuity. It is made available under a CC-BY-NC-ND 4.0 International license .

Table 1: Key parameters used in the Matlab® simulation of the HAFB wastewater network.

Category	Parameter	Value(s)
Pathogen	Shed rate (SARS-CoV-2)	$10^{7.53}$ – $10^{9.27}$ gc/g-feces [41]
	WW degradation coefficient	1.752 day^{-1} [42]
Source	Mean fecal mass	120 g [43]
	Pulse duration	10 - 40sec
	Pulse frequency	1.2 day^{-1}
Hydraulic	Manning roughness	0.01 – 0.019 $s/m^{1/3}$
	Pipe slope	0.02 m/m
	Dispersion coefficient	0.009 – 0.374 m^2/s
	Pump station wet well volume	5200 gal (max 10,000 gal)
Simulation	Time step	5 s
	Simulation duration	5 h

Estimated Detection Platform Operational LOD

Concentration profiles were generated by the model in units of gene copies per unit volume (gc/mL) to allow easy conversion between target organisms with differing genome sizes. LODs for various sequencing platforms are not specified by the manufacturer, as LOD varies with factors including sample background, target, lab processing methods and data analysis methods; rather, a minimum input mass is recommended by the manufacturer for sequencing library preparation. To estimate the detection technology's LOD requires the conversion from minimum input mass to gc/mL. Assumptions about sample volumes at various stages of the preparation process, genome size of the target organism and amount of target contained in the input mass can yield a theoretical minimum input for mNGS. In this study, using SARS-CoV-2 as a representative pathogen, and accounting for pragmatic recovery efficiencies along the

medRxiv preprint doi: https://doi.org/10.64898/2026.08.18.26360688; this version posted August 21, 2026. The copyright holder for this preprint
(which was not certified by peer review) is the author/funder, who has granted medRxiv a license to display the preprint in perpetuity.
It is made available under a CC-BY-NC-ND 4.0 International license .

160 way, this input mass is adjusted and referred to as the *realistic minimum input*. These assumptions are listed
161 in Table 2**.** Table 3 summarizes the estimated theoretical and realistic platform minimum inputs for three
162 different detection technologies.

163 **Table 2: Key assumptions for mass to gc/mL conversion.**

SARS-CoV-2 genome size[44]	~29,900 RNA bases
Overall recovery efficiency at *each* of 4 steps of processing	10%
Target mass contributing to minimum input mass	1%
Sample volume processed for sequencing	300 mL
Reaction volume for qPCR	50 µL
Amplification bias	Not considered
SARS-CoV-2 shed rate[45]	10^7 - 10^9 gc/g-feces
Target mass per flush (120 g stool containing 10^9 gc/g)[46]	1.2×10^{11} gc

164

medRxiv preprint doi: https://doi.org/10.64898/2026.08.18.26360688; this version posted August 21, 2026. The copyright holder for this preprint (which was not certified by peer review) is the author/funder, who has granted medRxiv a license to display the preprint in perpetuity. It is made available under a CC-BY-NC-ND 4.0 International license .

Table 3: Estimated minimum input in gc/mL for select detection technologies.

Technology	Library Prep Protocol	Minimum Input	Theoretical Estimated Minimum Input (target gc/mL)	Realistic Estimated Minimum Input (target gc/mL
Oxford Nanopore MinION (sequencing)	Ligation Sequencing Kit	1,000 ng[47]	2.1×10^{7}	2.1×10^{10}
Illumina NextSeq550 (sequencing)	Illumina DNA Prep	1 ng[48]	2.1×10^{4}	2.1×10^{7}
Applied Biosystems QuantStudio7 (quantitative PCR)	N/A	80 gc/mL[49]	80	80

Preparation of spike in bacteria for laboratory and system spike experiments

Atlantibacter subterraneus (Asub - formerly known as *Salmonella subterranea*) was selected for the laboratory and system spike experiments due to its ease of propagation in large volumes and low background presence in Kraken2 analysis of previous HAFB wastewater samples. A freeze-dried bacterial strain of Asub was purchased from ATCC (ATCC BAA-836) and rehydrated following ATCC handling instructions. The rehydrated bacteria were streaked onto Tryptic Soy Agar (TSA) plates to obtain single colonies. Individual colonies were used to inoculate multiple Tryptic Soy Broth (TSB) cultures, which were incubated overnight at 35 °C with aeration. Glycerol stocks were prepared by adding 500 µL of the culture to 500 µL of sterile filtered 50% glycerol in cryovials for storage at -80 °C.

For preparation of bacteria for system spike in experiments, bacteria growth was scaled up across multiple days in shake flasks and incubated at 35 °C shaking from 150-250 RPM based on the size of the

medRxiv preprint doi: https://doi.org/10.64898/2026.08.18.26360688; this version posted August 21, 2026. The copyright holder for this preprint
(which was not certified by peer review) is the author/funder, who has granted medRxiv a license to display the preprint in perpetuity.
It is made available under a CC-BY-NC-ND 4.0 International license .

flask. On the starting date, multiple 5 mL cultures were started from glycerol stocks of Asub and incubated for 24 hours before pooling and adding to a 150 mL TSB culture. These cultures were incubated for another 24 hours before back dilution and split into multiple 500 mL cultures. After another 24 hours of growth, approximately 2 L of bacteria were available for the system spike-in. The cumulative time to grow up this material was approximately 72 hours. The optical density at 600 nm (OD600) of the culture was measured throughout the growing process. The procedure for preparing bacteria for the laboratory spike was similar to above, but due to lower total culture volumes needed, cultures were incubated for 24 hours only.

Heat inactivation of bacteria before system spikes

Bacteria were required to be 100% inactivated before spiking into the sewer system based on our organization's Environment, Health, and Safety (EHS) department and public works guidelines. Heat treatment at 90 ℃ for 15 minutes in a water bath was shown to fully inactivate bacteria and minimally impact downstream molecular detection. The heat-inactivated bacteria were streaked onto TSA plates and left to incubate overnight at 35 ℃ to verify inactivation.

Quantification of bacteria preparations

A qPCR assay was designed to quantify genomic copy numbers of Asub. Primer and probe sequences are listed in Table S2. This assay was tested against a positive control DNA fragment (DedA - Integrated DNA Technologies) and nucleic acids extracted from culture using the Qiagen DNeasy PowerSoil Kit (Qiagen 12855-100). To create a standard curve, twelve samples from a 10-fold dilution series of the extracted culture in nuclease free water were tested in duplicate using the Luna Universal qPCR Master Mix (NEB M3003X). 2 µL of sample was added to 10 µL of master mix, 1 µL of the PrimeTime qPCR custom assay (20×) and 7 µL of nuclease free water. Cycling parameters were as follows: 95 ℃ for 20 s, followed by 40 cycles of denaturing at 95 ℃ for 3 s and annealing/extension at 60 ℃ for 30 s on a Thermo Fisher QuantStudio 7 Pro. To determine the LOD of the qPCR assay, 20 replicates were tested and

medRxiv preprint doi: https://doi.org/10.64898/2026.08.18.26360688; this version posted August 21, 2026. The copyright holder for this preprint (which was not certified by peer review) is the author/funder, who has granted medRxiv a license to display the preprint in perpetuity. It is made available under a CC-BY-NC-ND 4.0 International license .

the concentration at which 19/20 replicates were positive was identified as the assay LOD (13 copies per reaction, Cq = 37.26)

The same 10-fold dilution series of the extracted culture was quantified by digital PCR (Qiagen QIAcuity) using the assays outlined above, the QIAcuity OneStep Advanced Probe Kit (Qiagen 250131) and the QIAcuity Nanoplate 8.5k 96-well plates (Qiagen 250021). 2 µL of sample were added to 3 µL One Step Advanced Probe Master Mix (4×), 0.6 µL of PrimeTime qPCR custom assay (20×), 1.5 µL of GC Enhancer and 4.9 µL of nuclease free water. Cycling parameters were as follows: 95 ℃ for 3 min, followed by 40 cycles of denaturing at 95 ℃ for 5 s and annealing/extension at 60 ℃ for 30 s. Standard curves were created by combining the results from the dPCR and qPCR experiments. The original concentration of the *Asub* culture was estimated by using the standard plate count method. A serial dilution of the culture was created and 100 µL of each dilution were plated on TSA plates and left to incubate overnight at 35 ℃. Colonies were enumerated and the colony-forming units (CFU)/mL in the starting culture was calculated. 1 mL of the culture was extracted using the Qiagen DNeasy PowerSoil Kit (Qiagen 12855-100), resulting in a final elution volume of 50 µL. With 2 µl added to each qPCR reaction, the CFU represented in each qPCR reaction was calculated and plotted against the qPCR cycle threshold values.

Laboratory spikes of bacteria into de-ionized water (DI) water and wastewater backgrounds

A 250 mL volume of wastewater was collected from a wastewater pump station in Lexington, MA. Samples were heat-inactivated within 15 min of collection at 60 °C for 60 min in a water bath. Asub was cultured and quantified as described above and spiked into 40 mL aliquots of either DI water or wastewater in a 10× dilution series. Nucleic acid extraction was conducted immediately using the Promega Wizard® Enviro Total Nucleic Acid Kit (Promega, A2991), with 40 mL input per the manufacturer's instructions. A 40 µL volume was used to elute the nucleic acids. All elutions were run through the *OneStep* PCR Inhibitor Removal Kit (Zymo Research D6031). Post-extraction elutions were quantified using the Qubit 1X dsDNA assay (ThermoFisher Scientific Q33231). qPCR assays targeting Asub and Tomato brown rugose fruit virus

medRxiv preprint doi: https://doi.org/10.64898/2026.08.18.26360688; this version posted August 21, 2026. The copyright holder for this preprint
(which was not certified by peer review) is the author/funder, who has granted medRxiv a license to display the preprint in perpetuity.
It is made available under a CC-BY-NC-ND 4.0 International license .

(ToBRFV) were conducted, and samples were sent for Illumina DNA sequencing by SeqCenter (Pittsburgh, PA, USA).

System spikes of bacteria into local wastewater network

Wastewater system spike-ins were conducted after acquiring approvals from the EHS team as well as local and greater Boston public works departments. Preliminary dye tests were performed to track timing of material from release point to collection point. 500 mL of fluorescent dye (USABlueBook® Sewer Tracing Dye, Yellow-Green Liquid) was released from the designated point and tracked at the collection point for transit time and visibility. The dye was determined not to interfere with downstream molecular analyses of the wastewater samples. For bacterial spikes, 500 mL of dye was mixed with 500-1250 mL of quantified heat-inactivated bacteria and released at the designated point, followed by 10 flushes. Wastewater samples were collected at the pump station after approximately 30 min; one 250 mL sample every minute until the dye was no longer visible. Eight bacterial spikes were conducted on four different days. Wastewater samples were transported to the lab, and sample processing and nucleic acid extraction were conducted as described above.

Illumina library preparation and sequencing

Extracted wastewater nucleic acids were sent to SeqCenter (Pittsburg, PA, USA) for Illumina library preparation and sequencing using the Illumina DNA Prep kit and custom IDT 10bp unique dual indices (UDI) with a target insert size of 280 base pairs (bp). Illumina sequencing was performed on an Illumina NovaSeq X Plus sequencer, producing 2×151 bp paired-end reads. Demultiplexing, quality control, and adapter trimming were performed with bcl-convert1 (v4.2.4).

ONT library preparation and sequencing

medRxiv preprint doi: https://doi.org/10.64898/2026.08.18.26360688; this version posted August 21, 2026. The copyright holder for this preprint (which was not certified by peer review) is the author/funder, who has granted medRxiv a license to display the preprint in perpetuity. It is made available under a CC-BY-NC-ND 4.0 International license .

Libraries were prepared for long-read sequencing using the ONT Native Barcoding Kit 24 V14 (SQK-NBD114.24) kit, per manufacturer's instructions. Samples were normalized to the lowest concentration and pooled after the addition of barcodes. Libraries were quantified using the Qubit assay (dsDNA HS, ThermoFisher) per the manufacturer's instructions. Pooled ONT libraries were sequenced using a dedicated PromethION flow cell at SeqCenter (Pittsburgh, PA, USA).

Bioinformatic analysis

Adaptor sequences and low-quality bases in Illumina reads were trimmed using BBduk[50] under default parameters (ktrim=r k=23 mink=11 hdist=1 tpe tbo). ONT pod5 files were basecalled and demultiplexed with dorado v1.1.0 and the dna_r10.4.1_e8.2_400bps_hac@v4.3.0 model. ONT reads were filtered with NanoFilt[51] to an average Phred score of 10 per read and minimum read length of 100 bp. Average data output post-QC for Illumina samples was 53 Gbp per sample (SD: 9.7 Gbp) and average data output post-QC for ONT samples was 3.4 Gbp per sample (SD: 1.4 Gbp). To facilitate comparisons between samples with varying sequencing output, each sample was subsampled to the lowest output found in the dataset (~1.2 Gbp per sample). A custom Kraken2[52] database composed of GTDB bacterial species, viral genomes from NCBI, CheckV, and EsViritu databases and eukaryotic pathogens from EuPathDB was used for read-based taxonomic classification. Minimap2[53] was used for read mapping to the Asub reference genome (https://genomes.atcc.org/genomes/c52b51a4132d47f0) or a combined reference that included the Asub genome and the *Atlantibacter hermanii* genome (NCBI RefSeq GCF_016027855) to understand the effect of including near-neighbors. The "sr" and "map-ont" parameters were used to map Illumina and ONT reads, respectively. Samtools[54] was used to calculate coverage and depth with mapping quality (min-MQ = 30) and base quality (min-BQ = 30) thresholds. Total mapped bases were calculated from the samtools depth output. GOTTCHA2[55] was used as another method to conduct species-specific read mapping. Bioinformatic analyses were conducted using high-performance computing resources from the MIT Lincoln Laboratory Supercomputing Center. [56]

medRxiv preprint doi: https://doi.org/10.64898/2026.08.18.26360688; this version posted August 21, 2026. The copyright holder for this preprint
(which was not certified by peer review) is the author/funder, who has granted medRxiv a license to display the preprint in perpetuity.
It is made available under a CC-BY-NC-ND 4.0 International license .

277

278 ***Calculating the Operational Limit of Detection (LOD) for mNGS-based WBS***

279 Bases mapped to the target by each bioinformatic tool were normalized by the number of bases
280 post-QC and multiplied by 1,000,000 to obtain mapped bases per million (MBPM). Within each spike
281 experiment, the MBPM of spiked samples was divided by the MBPM of the no-spike background samples
282 to obtain MBPM over background, which is analogous to a signal to noise ratio (SNR). A threshold was
283 established by computing the average MBPM over background of non-spiked samples ± 3 standard
284 deviations to account for the high variability of wastewater samples. The operational LOD was determined
285 to be the concentration of spiked target where MBPM over background exceeded the threshold consistently
286 across all 4 spike experiments. In cases where there was no target detection in the blank, mapped bases = 1
287 was used for the analysis.

288

289 ***Permutation Testing for MBPM over background of Illumina vs ONT sequencing***

290 For each bioinformatic analysis method, samples with paired Illumina and ONT sequencing were
291 selected for permutation testing. The test statistic for the observed data was calculated as follows:

292 1. Calculation of the difference between the log of the Illumina MBPM over background and the log
293 of the ONT MBPM over background. Log transform prior to differencing was chosen to account
294 for the fact that MBPM over background is a ratio.
295 2. Average of the difference within spike experiments, to account for the grouped structure
296 3. Average of the averages across spike experiments, to account for the grouped structure

297 Furthermore, 20,000 permutations of the sign of the differences were conducted and the test statistic
298 was calculated as described above to form a null distribution. The two-tailed p-value was calculated as the
299 number of permuted statistics that were equal to or more extreme than the observed test statistic. When no
300 permutations resulted in a test statistic more extreme than the observed test statistic, the p-value is reported
301 as $p<5.0 \times 10^{-5}$ (1/20,000).

medRxiv preprint doi: https://doi.org/10.64898/2026.08.18.26360688; this version posted August 21, 2026. The copyright holder for this preprint
(which was not certified by peer review) is the author/funder, who has granted medRxiv a license to display the preprint in perpetuity.
It is made available under a CC-BY-NC-ND 4.0 International license .

RESULTS

WW model-based sampling architecture assessment suggests that qPCR monitoring is more sensitive than mNGS for base-level sampling

Three different sampling approaches were examined: monitoring a large installation while sampling at key aggregation points only (two samples each from lower and upper pump station wet well), sampling multiple branches within the installation to improve source localization (ten samples) and sampling outside of each building (100+ samples) to provide the highest level of spatial resolution. Several model simulations were performed varying the number of infected contributors and location sources. 71 scenarios examined a single infected person at each of the simplified model nodes. Estimated detection results for the single shedder scenarios under the three different sampling approaches are shown in Figure 1. A qPCR detection platform shows an estimated minimum input of ~10^2 gc/mL, while estimated values of the Illumina and ONT MinION platforms show ~10^7 and 10^{11} respectively. With qPCR as a detection platform, the base can be effectively monitored from two sampling locations with the exception being contributions from sources at the most distal ends of the system. Randomly sampling at branches may result in detection with some sequencing platforms although full network coverage is lost unless every branch is included. Random sampling from each building yields high enough concentrations to be detected robustly.

medRxiv preprint doi: https://doi.org/10.64898/2026.08.18.26360688; this version posted August 21, 2026. The copyright holder for this preprint
(which was not certified by peer review) is the author/funder, who has granted medRxiv a license to display the preprint in perpetuity.
It is made available under a CC-BY-NC-ND 4.0 International license .

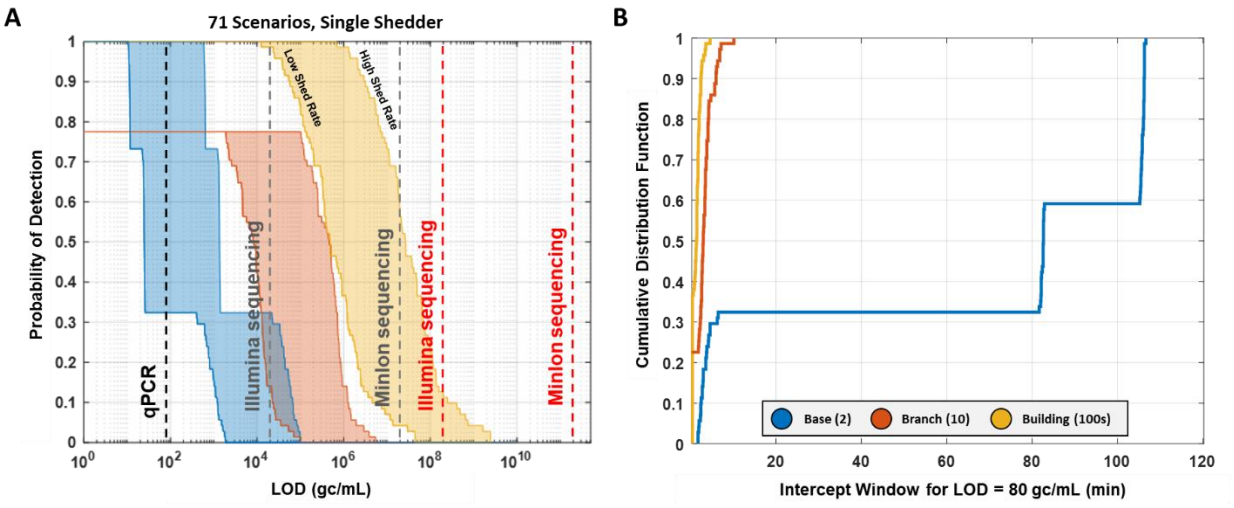


Figure 1: Computational model enables estimation of wastewater surveillance feasibility of different sampling architectures and detection technologies. (A) LOD (estimated mass input) as a function of probability of detection (detectable scenarios) across single shedder simulations. Vertical lines denote estimated detection threshold ranges with a particular detection platform (subject to the assumptions described in the Methods section) at high and low shed rates. Gray = theoretical, red = realistic estimated minimum input. (B) Amount of time in minutes that concentration is above qPCR threshold for the different sampling approaches with a single high shedder at various locations within the network.

Successful detection also requires that the sample can be effectively collected for analysis. The amount of time a sample is above LOD (i.e., dwell time or window to intercept detectable sample) is shown for the most sensitive detection platform (qPCR) in Figure 1. Although overall sample concentrations are lower at the pump station wet wells, they persist much longer than that of the highly transitory pipes and manholes within the system. Unless nearly continuous sampling was implemented, the target could be missed entirely if sampling from pipes and manholes.

Table S3 contains a summary of parameters that affect an overall sampling architecture: sample numbers (a driver of program cost) and detection (ability to acquire sample and detect target). The ONT MinION platform was excluded as no scenario with realistic estimated minimum input was predicted to be

medRxiv preprint doi: https://doi.org/10.64898/2026.08.18.26360688; this version posted August 21, 2026. The copyright holder for this preprint
(which was not certified by peer review) is the author/funder, who has granted medRxiv a license to display the preprint in perpetuity.
It is made available under a CC-BY-NC-ND 4.0 International license .

336 detectable. These initial modeling estimates helped to guide when and where to sample within the HAFB
337 wastewater network as well as inform expectations for detection with different mNGS platforms. The model
338 developed can be updated with actual dilution and transit times should a more accurate predictive capability
339 be required. The model can also be adapted quickly to represent other wastewater networks.
340
341 ***Lab-based spike of A. subterraneus cells into DI water and wastewater sample matrix reveal different***
342 ***LODs for qPCR, Illumina, and ONT sequencing***
343 The computational model highlighted different LODs for qPCR and sequencing but was based on
344 extensive assumptions. To empirically determine the operational LOD, we conducted lab-based spike
345 experiments where whole Asub cells were spiked into wastewater and DI water prior to extraction and
346 molecular detection. The operational LOD of qPCR for DI water and wastewater spikes was determined to
347 be between 150 – 1,500 CFU/mL over background (Figure 2A). This result was consistent with the qPCR
348 assay validation testing, which showed an assay LOD of 13 copies per reaction, corresponding to Cq=37.26.
349 The targeted nature of qPCR suggests that the background matrix should not impact the LOD of the assay.
350 The qPCR detections of lab-based spiked wastewater samples were used to generate a standard curve which
351 could be used to estimate the concentration of the spiked target in the later wastewater system spike
352 experiments (Figure S4).

medRxiv preprint doi: https://doi.org/10.64898/2026.08.18.26360688; this version posted August 21, 2026. The copyright holder for this preprint
(which was not certified by peer review) is the author/funder, who has granted medRxiv a license to display the preprint in perpetuity.
It is made available under a CC-BY-NC-ND 4.0 International license .

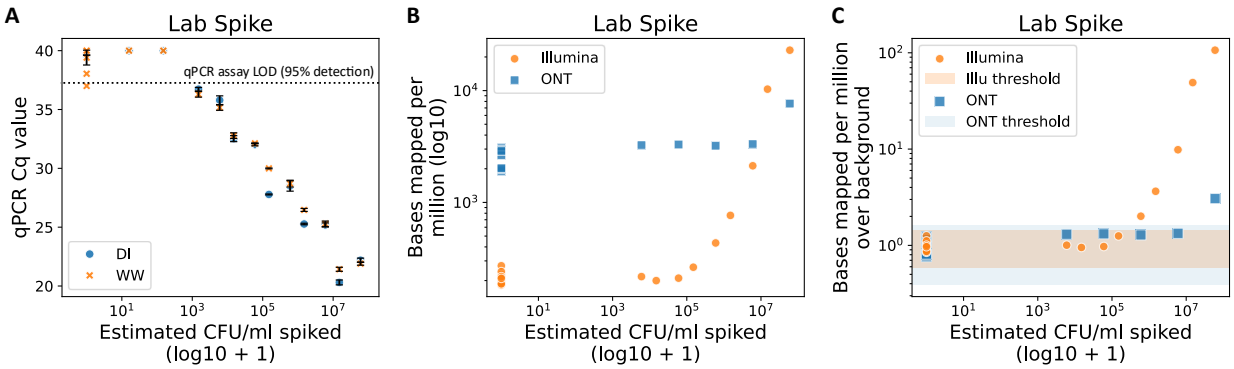


Figure 2: Laboratory spike-in experiments. (A) qPCR detection of Asub cells spiked into DI water and wastewater backgrounds. Asub cells were quantified by plating, then spiked into DI water and wastewater samples before nucleic acid extraction and qPCR. qPCR assay validation showed an assay LOD of 13 copies/reaction, corresponding to Cq=37.26. Samples with no qPCR detection were assigned Cq=40. X-axis has a pseudocount of 1 added to visualize blanks on a log scale. **(B)** mNGS detection of Asub cells spiked into DI water and wastewater in the lab on Illumina and ONT platforms. Y-axis represents the number of bases mapped to the Asub reference genome by minimap2 normalized by the total number of bases after quality control, multiplied by a factor of 10^6. X-axis has a pseudocount of 1 added to visualize blanks on a log scale. **(C)** mNGS detection of *Asub* cells spiked into DI water and wastewater in the lab on Illumina and ONT platforms. Y-axis represents the ratio between the MBPM of the sample compared to the blank. X-axis has a pseudocount of 1 added to visualize blanks on a log scale. Shaded regions in light orange and light blue represent the average MBPM of the blank samples +/- 3 standard deviations for Illumina and ONT, respectively. CFU: colony forming units. DI: deionized water. WW: wastewater. Cq: quantification cycle. MBPM: mapped bases per million, number of bases mapped to the target organism normalized by the number of bases after sequencing read quality control and multiplied by a factor of 10^6

Wastewater samples spiked with Asub cells were also characterized with mNGS on Illumina and ONT platforms. Illumina data showed a higher target signal than ONT data at high spike concentrations as

medRxiv preprint doi: https://doi.org/10.64898/2026.08.18.26360688; this version posted August 21, 2026. The copyright holder for this preprint
(which was not certified by peer review) is the author/funder, who has granted medRxiv a license to display the preprint in perpetuity.
It is made available under a CC-BY-NC-ND 4.0 International license .

372 measured by mapped bases per million (MBPM) (Figure 2B). ONT data showed a higher background signal
373 than Illumina data, where samples without any target spike-in showed ~3000 MBPM (Figure 2B). Taken
374 together, these observations highlight that Illumina has a higher signal to noise ratio than ONT for this
375 experiment (Figure 2C). The threshold for detection was set as the average MBPM of no-spike wastewater
376 samples + 3 standard deviations. Based on these thresholds, the operational LOD of Illumina sequencing
377 was determined to be between 1.5×10^5 and 6.0×10^5 CFU/mL wastewater, whereas the operational LOD
378 of ONT sequencing was determined to be between 6.0×10^5 and 6.0×10^6 CFU/mL wastewater.
379
380 ***qPCR detection for wastewater system spike shows background interference***
381 The lab spiking results did not consider the loss of material and dilution that occurs in a real-world
382 sewer network. To understand how the sewer network can influence the operational LOD, we ran several
383 experiments where we spiked the HAFB sewer system with Asub combined with fluorescent dye. The dye
384 and microbial spike were shown to transit the system together (Figure S2). qPCR detection from the system
385 spike experiments is shown in Figure 3. The qPCR assay can detect ~300 CFU/mL in wastewater, consistent
386 with the lab-based spike results, but endogenous Asub signal in the wastewater background makes the
387 spiked signal indistinguishable from noise until $\sim 1.3 \times 10^5 - 3.6 \times 10^5$ CFU/mL wastewater. This
388 operational LOD is higher than that reported for the lab-based spike (150 – 1,500 CFU/mL wastewater,
389 Figure 2A), which could be due to variable wastewater backgrounds during the months that the system
390 spike experiments were conducted.

medRxiv preprint doi: https://doi.org/10.64898/2026.08.18.26360688; this version posted August 21, 2026. The copyright holder for this preprint
(which was not certified by peer review) is the author/funder, who has granted medRxiv a license to display the preprint in perpetuity.
It is made available under a CC-BY-NC-ND 4.0 International license .

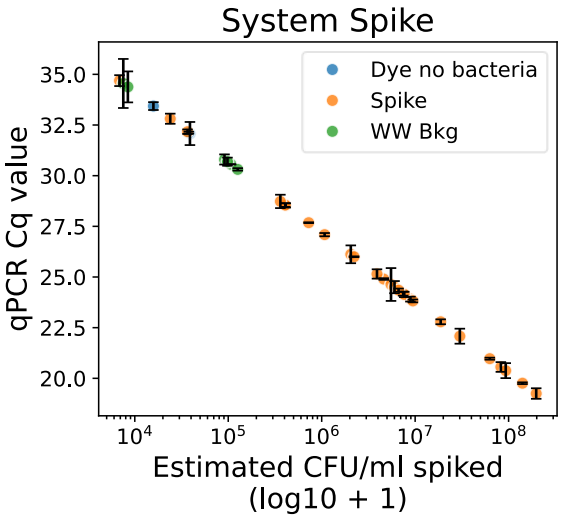


Figure 3: qPCR detection of wastewater system spike. Asub was flushed into the wastewater system. Wastewater samples were collected at the pump station, assayed with qPCR, and CFU/mL in the sample was estimated based on the standard curve in Figure S4. WW bkg: wastewater background before target was spiked. Dye no bacteria: wastewater background with fluorescent dye only, without target bacteria. Spike: samples collected after target bacteria were spiked in the sewer system. CFU: colony forming units. Cq: quantification cycle

Bioinformatic methods that use species-specific databases enhance signal to noise ratio in mNGS detection of spiked target in wastewater.

Because different bioinformatic methods have been shown to have different performance characteristics[57], we used different bioinformatic methods to analyze the wastewater system spike samples and understand the effect on mNGS detection. We measure detection with the estimated operational LOD as well as the MBPM over background metric, which is analogous to a signal to noise ratio (SNR). Minimap2 mapping of reads to the Asub genome alone showed that detection above background became consistent after the spike concentration exceeded ~7.6×10^6 CFU/mL wastewater for Illumina data and ~6.3×10^7 CFU/mL wastewater for ONT data (Figure S5, Figure S6). We further investigated the effect of

medRxiv preprint doi: https://doi.org/10.64898/2026.08.18.26360688; this version posted August 21, 2026. The copyright holder for this preprint (which was not certified by peer review) is the author/funder, who has granted medRxiv a license to display the preprint in perpetuity. It is made available under a CC-BY-NC-ND 4.0 International license .

adding an *A. hermannii* (Aherm) reference genome in addition to the target Asub to the mapping process. The minimap2 results with a two-genome reference showed slightly improved estimated operational LOD for ONT (Figure 4A) and slightly improved SNR compared to the results with only the target genome (Figure S5, Figure S6). As an alternative method, Kraken2 was used to investigate the effect of taxonomic classification with a broad database. With Kraken2, operational LOD decreased to ~4.1×10^5 CFU/mL wastewater for Illumina data and ~9.5×10^6 CFU/mL wastewater for ONT data (Figure 4A, Figure S5, Figure S6). Kraken2 further increased SNR for Illumina and ONT data (Figure 4B). Finally, GOTTCHA2 with a broad database was used to map reads against species-specific markers. While operational LOD for GOTTCHA2 analysis was similar to Kraken2 analysis for both Illumina and ONT (Figure 4A), GOTTCHA2 had the highest SNR of all assessed methods (Figure 4B, Figure S5, Figure S6). There is a statistically significant difference in the average MBPM over background for Illumina-sequenced samples compared to ONT-sequenced samples (two-tailed permutation test, Figure 4B). We observe that the MBPM over background metric is higher for Illumina (Figure 4B,D) and the operational LOD is lower for Illumina (Figure 4A,C), with and without subsampling the data to match the lowest ONT sample's sequencing output.

Using the lowest dilution factor for a spiked sample (~5000×, measured by fluorescent dye), the shed rate of Salmonella in animal models (~10^2 – 10^7 CFU/g feces),[58] and assuming 1 g feces corresponds to 1 mL, the lowest estimated operational LOD (~4.1×10^5 CFU/mL) corresponds to 2×10^2 – 2×10^7 people with Salmonella infection. This estimate assumes that all material is discharged from one point in the system at once, which is unlikely. Further modeling would be necessary to include variation related to outbreak progression and random toilet usage.

medRxiv preprint doi: https://doi.org/10.64898/2026.08.18.26360688; this version posted August 21, 2026. The copyright holder for this preprint
(which was not certified by peer review) is the author/funder, who has granted medRxiv a license to display the preprint in perpetuity.
It is made available under a CC-BY-NC-ND 4.0 International license .

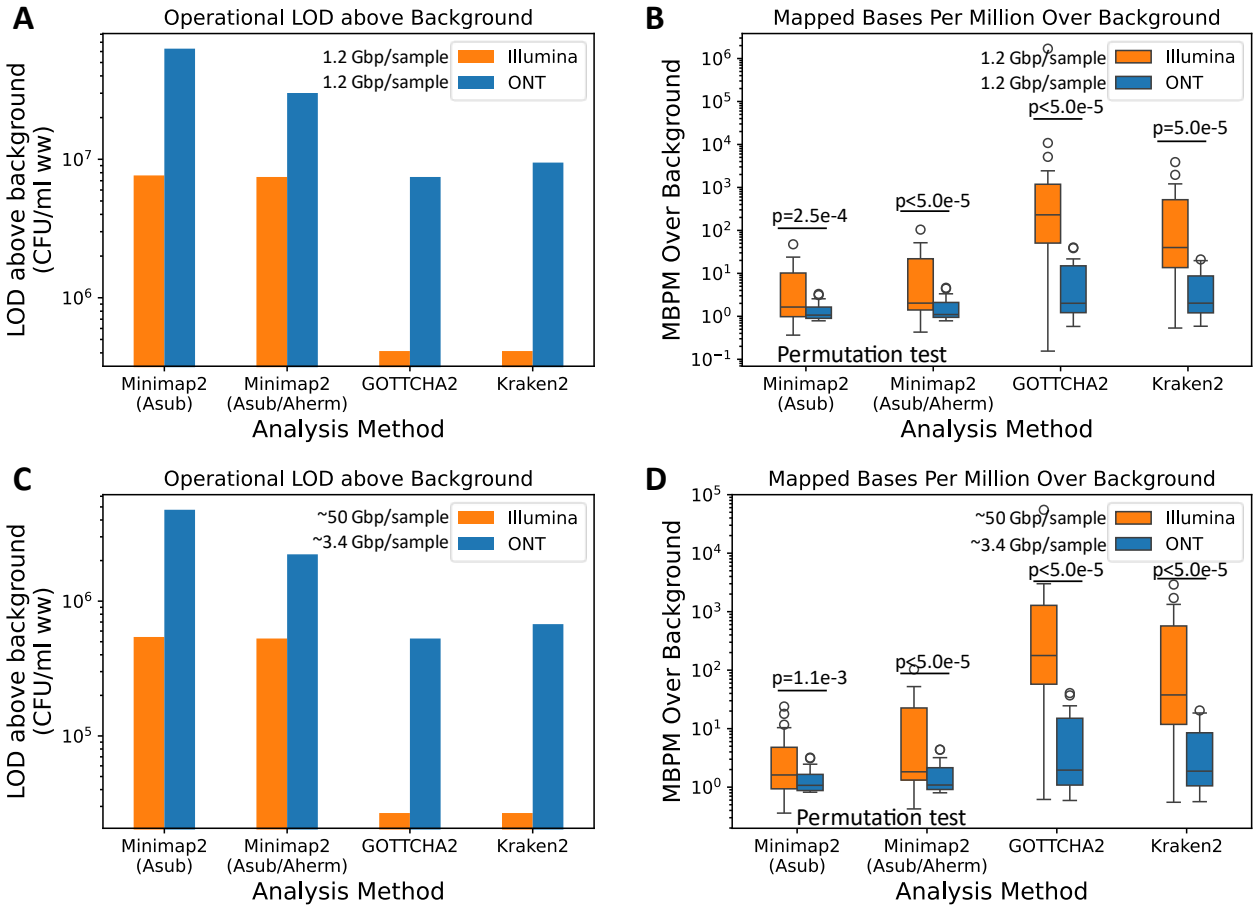


Figure 4: Summary of LOD and SNR for different sequencing and bioinformatic methods, with and without subsampling. (A) Limit of detection ranges identified through system-spike experiments for Illumina and ONT datasets analyzed with different bioinformatic methods, all samples subsampled to 1.2 Gbp sequencing output. **(B)** Distribution of MBPM over background values for spike samples, sequenced with Illumina and ONT and analyzed with different bioinformatic methods, all samples subsampled to 1.2 Gbp sequencing output. **(C)** Limit of detection ranges identified through system-spike experiments for Illumina and ONT datasets analyzed with different bioinformatic methods, all samples subsampled to 1.2 Gbp sequencing output, without subsampling. **(D)** Distribution of MBPM over background values for spike samples, sequenced with Illumina and ONT and analyzed with different bioinformatic methods, without subsampling. LOD: limit of detection. SNR: signal to noise ratio. MBPM: mapped bases per

medRxiv preprint doi: https://doi.org/10.64898/2026.08.18.26360688; this version posted August 21, 2026. The copyright holder for this preprint
(which was not certified by peer review) is the author/funder, who has granted medRxiv a license to display the preprint in perpetuity.
It is made available under a CC-BY-NC-ND 4.0 International license .

440 million, number of bases mapped to the target organism normalized by the number of bases after
441 sequencing read quality control and multiplied by a factor of 10^6. Asub: *Atlantibacter subterraneus*.
442 Aherm: *Atlantibacter hermannii.*
443

444 **DISCUSSION**

445 There is a rising interest in using increasingly agnostic detection methods such as mNGS to detect
446 and identify pathogens, including those that may be genetically modified, emerging or novel. However,
447 applying mNGS to operational WBS requires an understanding of its performance metrics at each location
448 and how mNGS information can be used to make actionable decisions. The LOD for a detection system is
449 critical information because it helps inform what a detection means in terms of quantity of potential
450 pathogen in the WW system. This information can then be used to infer how many people may be infected
451 and thus the severity of the pathogen spread. Knowledge of system LOD enables the decision maker to
452 determine the appropriate level of response and risk for a particular community. Here, we describe a process
453 for establishing an mNGS LOD for wastewater surveillance at a military base through computational
454 modeling and experimentally-derived results.

455 A simplified hydraulic model based on SARS-CoV-2 predicted that mNGS would be less sensitive
456 than qPCR for detecting single cases. The computational model included many simplifications of the
457 variations in system design parameters, flow rates, sampling type, sample processing methodology and
458 sequencing methods. We chose many parameters based on vendor information, available research, and
459 knowledge of the system gained by design documents. Even with all this information, it is difficult to create
460 an exact duplication of the wastewater system due to complex aspects of the hydraulic environment,
461 including the system turbulence, inflow and infiltration, degree of biofilm built up on pipe walls, and
462 variations in daily usage. Potential improvements to the model include estimating inflow and infiltration,
463 adding a time-dependent water usage parameter, and fine-tuning wastewater system design parameters
464 based on dye testing results. The modeling framework described here can be used as a preliminary

medRxiv preprint doi: https://doi.org/10.64898/2026.08.18.26360688; this version posted August 21, 2026. The copyright holder for this preprint (which was not certified by peer review) is the author/funder, who has granted medRxiv a license to display the preprint in perpetuity. It is made available under a CC-BY-NC-ND 4.0 International license .

feasibility assessment when establishing new WBS locations, although location-specific inputs, including wastewater system design and flow rates, will be necessary to tailor results.

Laboratory and wastewater system-based spike experiments assessed how the wastewater sample matrix influences detection limits due to existing microbial content and assay interferents. Operational LOD is primarily affected by the level and variability of target detected in the background sample. Operational LODs for mNGS methods were equivalent to or higher than the qPCR operational LOD, depending upon sequencing and bioinformatics methods. Illumina sequencing outperformed ONT sequencing, with a ~70× lower operational LOD for some analysis methods. Elevated operational LOD for ONT could be caused by inaccurate read mapping. ONT has been shown to have a higher sequencing error rate than Illumina[59], which could increase background and decrease target-specific mapping. We observed that the application of the minimap2 algorithm to long vs. short reads generated from identical input samples resulted in a log difference in the signal to noise ratio for some methods, which could be due to different default parameters within the software. Finally, whereas ONT sequencing typically has longer read lengths that could increase confidence in target-specific mapping, nucleic acids could degrade in the wastewater due to environmental and chemical factors as well as during sample processing manipulations. We observe that average ONT read lengths from the spike samples are similar to those of Illumina (Figure S3), which may offset potential advantages of long reads for species-specific identification.

The differences between the model-predicted and the experimentally-derived operational LODs can be attributed to several factors. First, the model assumptions were based on the SARS-CoV-2 virus (genome size ~29,900 bases), whereas the experiments were conducted with the Gram-negative bacteria, Asub (genome size ~4.8 Mb). Differences in target organism affect recovery rates during sample processing as well as the relative mass of the target genome compared to the total wastewater nucleic acid output[60]. Accounting for differences in genome length and dsDNA vs ssRNA, the same number of genome copies of Asub is expected to contribute ~318× more nucleic acid content than SARS-CoV-2. The SARS-CoV-2-based model did not consider how the presence of near-neighbor organisms in the wastewater background

medRxiv preprint doi: https://doi.org/10.64898/2026.08.18.26360688; this version posted August 21, 2026. The copyright holder for this preprint
(which was not certified by peer review) is the author/funder, who has granted medRxiv a license to display the preprint in perpetuity.
It is made available under a CC-BY-NC-ND 4.0 International license .

would elevate the operational LOD, whereas the experimental results showed non-negligible background signal depending on analysis method. Second, the model assumed that 1% relative abundance of the target among the background was necessary for a confident sequencing detection without specifically considering sequencing output or bioinformatic analysis method. The experimental samples were sequenced deeply and subsampled to 1.2 Gbp per sample for fair comparison to the lowest output sample, and multiple analysis methods were used, many of which require less than 1% relative abundance for a detection.

As mNGS is increasingly incorporated into WBS efforts, it is vital to understand how decision makers would like to use this information to make choices. Discussions with the larger wastewater biosurveillance community (civilian and military) suggest that agnostic detection and identification capabilities for early warning would likely be employed alongside targeted quantitative methods particularly when so much is still unknown about the capability. To move towards operationality, a distributed WBS architecture using mNGS benefits from: standardized protocols (sampling, processing and analysis pipelines), information quality measures (contextual LOD and identification confidence) and knowledge of the normal WW background per region (contributing populations, dilution, diversity trends and inhibitors). Site-specific verification of best methods should be conducted when standing up new wastewater surveillance locations and modalities, and our results provide preliminary evidence for including certain methods when testing mNGS-based WBS. It is also critical to understand how methodological choices in a WBS mNGS workflow, including sample collection, extraction of nucleic acids, sequencing library preparation, sequencing platform and bioinformatic analysis of the resultant data affect operational LOD. There is currently no single gold-standard end-to-end workflow defined for mNGS, and variables throughout the workflow can introduce bias and impact results.[61,62,63,64] As mNGS approaches are more broadly deployed, there is a continued need to understand how workflow variables affect expected outcomes and performance in order to compare and contrast results from similar use cases.

Collectively, this study provides an example of how modeling and experimental approaches can be used to characterize the operational LOD for mNGS in wastewater samples. We provide insights into how

medRxiv preprint doi: https://doi.org/10.64898/2026.08.18.26360688; this version posted August 21, 2026. The copyright holder for this preprint
(which was not certified by peer review) is the author/funder, who has granted medRxiv a license to display the preprint in perpetuity.
It is made available under a CC-BY-NC-ND 4.0 International license .

the target concentration, background composition, bioinformatic algorithms and sequencing parameters affect the results of mNGS-based target detection. Subsequent work could include viral and Gram-positive bacteria spike experiments to further investigate the effects of process recovery and background noise. Other sample processing variations, such as depletion or enrichment, could be explored for potential operational LOD benefits or biases. Additional experiments in collaboration with other laboratories could be performed to assess sample-to-sample and lab-to-lab variability and gain more confidence in results. As WBS moves towards untargeted approaches like mNGS, the characterization of performance metrics using the process outlined here will be critical to gain decision maker confidence and enable actionable decision-making.

ACKNOWLEDGMENTS

We thank Stephen Francesconi (Defense Threat Reduction Agency) for helpful discussion and for sponsoring this work; Emily Kurdzo, Johanna Bobrow, Charlie Sinkler, Dave Walsh, Diane Jamrog and Henry Lau (MIT Lincoln Laboratory) for early thoughts on sample collection and processing; Jessie Hendricks (MIT Lincoln Laboratory) for advice on statistical analysis and permutation testing; David Wong and engineering team (Hanscom Air Force Base) for their help with sewer system maps and access to wastewater sampling sites; Nicholas Sevarino and Allison Heil (Weston and Sampson Engineers) for helping with the pilot dye test; Michael McLaren and William Bradshaw (SecureBio) for helpful discussion and advice on seeking permissions for spike experiments; Fred Sonnenwald and Ian Guymer (University of Sheffield) for helpful discussion on computational modeling.

medRxiv preprint doi: https://doi.org/10.64898/2026.08.18.26360688; this version posted August 21, 2026. The copyright holder for this preprint
(which was not certified by peer review) is the author/funder, who has granted medRxiv a license to display the preprint in perpetuity.
It is made available under a CC-BY-NC-ND 4.0 International license .

535 **REFERENCES**

1 Bar-Or I., Yaniv K., Shagan M., Ozer E., Erster O., Mendelson E., Mannasse B., Shirazi R., Kramarsky-Winter E., Nir O., Abu-Ali H., Ronen Z., Rinott E., Lewis Y.E., Friedler E., Paitan Y., Bitkover E., Berchenko Y., Kushmaro A. Regressing SARS-CoV-2 sewage measurements onto COVID-19 burden in the population: a proof-of-concept for quantitative environmental surveillance. medRxiv. 2020 doi: 10.1101/2020.04.26.20073569.

2 Kocamemi B.A., Kurt H., Hacioglu S., Yarali C., Saatci A.M., Pakdemirli B. First Data-Set on SARS-CoV-2 Detection for Istanbul Wastewaters in Turkey. medRxiv. 2020 doi: 10.1101/2020.05.03.20089417.

3 Medema G., Heijnen L., Elsinga G., Italiaander R., Brouwer A. Presence of SARS-Coronavirus-2 RNA in sewage and correlation with reported COVID-19 prevalence in the early stage of the epidemic in The Netherlands. Environ. Sci. Technol. Lett. 2020;7:511–516. doi: 10.1021/acs.estlett.0c00357.

4 Randazzo W., Truchado P., Cuevas-Ferrando E., Simón P., Allende A., Sánchez G. SARS-CoV-2 RNA in wastewater anticipated COVID-19 occurrence in a low prevalence area. Water Res. 2020;181 doi: 10.1016/j.watres.2020.115942.

5 Wurtzer S., Marechal V., Mouchel J.-.M., Maday Y., Teyssou R., Richard E., Almayrac J.L., Moulin L. Evaluation of lockdown impact on SARS-CoV-2 dynamics through viral genome quantification in Paris wastewaters. medRxiv. 2020 doi: 10.1101/2020.04.12.20062679.

6 Peccia J., Zulli A., Brackney D.E., Grubaugh N.D., Kaplan E.H., Casanovas-Massana A., Ko A.I., Malik A.A., Wang D., Wang M., Warren J.L., Weinberger D.M., Arnold W., Omer S.B. Measurement of SARS-CoV-2 RNA in wastewater tracks community infection dynamics. Nat. Biotechnol. 2020;38:1164–1167.doi:10.1038/s41587-020-0684-z.

7 Randazzo W., Truchado P., Cuevas-Ferrando E., Simón P., Allende A., Sánchez G. SARS-CoV-2 RNA in wastewater anticipated COVID-19 occurrence in a low prevalence area. Water Res. 2020;181 doi: 10.1016/j.watres.2020.115942.

8 Wu F., Zhang J., Xiao A., Gu X., Lee W.L., Armas F., Kauffman K., Hanage W., Matus M., Ghaeli N., Endo N., Duvallet C., Poyet M., Moniz K., Washburne A.D., Erickson T., Chai P., Thompson J., Alm E. SARS-CoV-2 titers in wastewater are higher than expected from clinically confirmed cases. mSystems. 2020;5:e00614–e00620. doi: 10.1128/mSystems.00614-20.

9 Wu F, Xiao A, Zhang J, Moniz K, Endo N, Armas F, Bonneau R, Brown MA, Bushman M, Chai PR, Duvallet C, Erickson TB, Foppe K, Ghaeli N, Gu X, Hanage WP, Huang KH, Lee WL, Matus M, McElroy KA, Nagler J, Rhode SF, Santillana M, Tucker JA, Wuertz S, Zhao S, Thompson J, Alm EJ. SARS-CoV-2 RNA concentrations in wastewater foreshadow dynamics and clinical presentation of new COVID-19 cases. Sci Total Environ. 2022 Jan 20;805:150121. doi: 10.1016/j.scitotenv.2021.150121. Epub 2021 Sep 4. PMID: 34534872; PMCID: PMC8416286.

medRxiv preprint doi: https://doi.org/10.64898/2026.08.18.26360688; this version posted August 21, 2026. The copyright holder for this preprint
(which was not certified by peer review) is the author/funder, who has granted medRxiv a license to display the preprint in perpetuity.
It is made available under a CC-BY-NC-ND 4.0 International license .

10 Adams C, Bias M, Welsh RM, Webb J, Reese H, Delgado S, Person J, West R, Shin S, Kirby A. The National Wastewater Surveillance System (NWSS): From inception to widespread coverage, 2020-2022, United States. Sci Total Environ. 2024 May 10;924:171566. doi: 10.1016/j.scitotenv.2024.171566. Epub 2024 Mar 9. PMID: 38461979; PMCID: PMC11103741.

11 Adams C, Bias M, Welsh RM, Webb J, Reese H, Delgado S, Person J, West R, Shin S, Kirby A. The National Wastewater Surveillance System (NWSS): From inception to widespread coverage, 2020-2022, United States. Sci Total Environ. 2024 May 10;924:171566. doi: 10.1016/j.scitotenv.2024.171566. Epub 2024 Mar 9. PMID: 38461979; PMCID: PMC11103741.

12 Kowallis WJ, Popelka SM, Millward GG, Penagosnino AS, Russell KR, Gutierrez AG, et al. Optimized methods for wastewater SARS-CoV-2 surveillance at military installations: Direct extraction showed higher recoveries relative to polyethylene glycol precipitation. Sci Tot Env. 2025 Jul 15;986:179759. doi: 10.1016/j.scitotenv.2025.179759.

13 Shu Y, McCauley J. GISAID: Global initiative on sharing all influenza data - from vision to reality. Euro Surveill. 2017 Mar 30;22(13):30494. doi: 10.2807/1560-7917.ES.2017.22.13.30494.

14 Fanelli A, Cescatti A, Ciscar J, Dubois G, Ibarreta D, Lowe R, et al. Assessing the risk of diseases with epidemic and pandemic potential in a changing world. Sci Adv. 2025 Jul 23;11(30): eadw6363. doi: 10.1126/sciadv.adw6363.

15 National Academies of Sciences, Engineering, and Medicine. Biodefense in the Age of Synthetic Biology. 2018. https://www.nationalacademies.org/read/24890

16 U.S. Department of Defense. Biodefense Posture Review. 2023. https://media.defense.gov/2023/Aug/17/2003282337/-1/-1/1/2023_biodefense_posture_review.pdf

17 Satam H, Joshi K, Mangrolia U, Waghoo S, Zaidi G, Rawool S, et al. Next-generation sequencing technology: Current trends and advancements. Biology (Basel). 2023 Jul 13;12(7):997. doi: 10.3390/biology12070997.

18 The Integrative HMP (iHMP) Research Network Consortium. The Integrative Human Microbiome Project. *Nature* **569**, 641–648 (2019). https://doi.org/10.1038/s41586-019-1238-8

19 Lloyd-Price, J., Mahurkar, A., Rahnavard, G. *et al.* Strains, functions and dynamics in the expanded Human Microbiome Project. *Nature* **550**, 61–66 (2017). https://doi.org/10.1038/nature23889

20 Martín R, Miquel S, Langella P, Bermúdez-Humarán LG. The role of metagenomics in understanding the human microbiome in health and disease. Virulence. 2014 Apr 1;5(3):413-23. doi: 10.4161/viru.27864. Epub 2014 Feb 11. PMID: 24429972; PMCID: PMC3979869.

21 Zhang L, Chen F, Zeng Z, Xu M, Sun F, Yang L, Bi X, Lin Y, Gao Y, Hao H, Yi W, Li M and Xie Y (2021) Advances in Metagenomics and Its Application in Environmental Microorganisms. Front. Microbiol. 12:766364. doi: 10.3389/fmicb.2021.766364

medRxiv preprint doi: https://doi.org/10.64898/2026.08.18.26360688; this version posted August 21, 2026. The copyright holder for this preprint
(which was not certified by peer review) is the author/funder, who has granted medRxiv a license to display the preprint in perpetuity.
It is made available under a CC-BY-NC-ND 4.0 International license .

22 Gomaa, E.Z. Human gut microbiota/microbiome in health and diseases: a review. *Antonie van Leeuwenhoek* **113**, 2019–2040 (2020). https://doi.org/10.1007/s10482-020-01474-7

23 Grice EA, Segre JA. The skin microbiome. Nat Rev Microbiol. 2011 Apr;9(4):244-53. doi: 10.1038/nrmicro2537. Erratum in: Nat Rev Microbiol. 2011 Aug;9(8):626. PMID: 21407241; PMCID: PMC3535073.

24 Rodrigo Mendes, Paolina Garbeva, Jos M. Raaijmakers, The rhizosphere microbiome: significance of plant beneficial, plant pathogenic, and human pathogenic microorganisms, *FEMS Microbiology Reviews*, Volume 37, Issue 5, September 2013, Pages 634–663, https://doi.org/10.1111/1574-6976.12028

25 Benoit P, Brazer N, de Lorenzi-Tognon M, Kelly E, Servellita V, Oseguera M, et al. Seven-year performance of a clinical metagenomic next-generation sequencing test for diagnosis of central nervous system infections. Nat Med. 2024 Dec;30(12):3522-3533. doi: 10.1038/s41591-024-03275-1.

26 Minogue TD, Koehler JW, Stefan CP, Conrad TA. Next-generation sequencing for biodefense: Biothreat detection, forensics, and the clinic. Clin Chem. 2019 Mar;65(3):383-392. doi: 10.1373/clinchem.2016.266536.

27 Sozhamannan S. Are we there yet? Agent agnostic metagenome sequencing for biothreat detection. Global Biodefense. 2024 Jul 31. Available from: http://globalbiodefense.com/2024/07/31/are-we-there-yet-agent-agnostic-metagenome-sequencing-for-biothreat-detection/.

28 Chiu CY, López-Labrador FX, Wilson MR, de Vries JJC. The regulatory landscape for clinical metagenomic testing. JAMA Neurol. 2025 Apr 7;82(8):761-762. doi: 10.1001/jamaneurol.2025.0461.

29 Child HT, Airey G, Maloney DM, Parker A, Wild J, McGinley S, et al. Comparison of metagenomic and targeted methods for sequencing human pathogenic viruses from wastewater. mBio. 2023 Dec 19;14:e01468-23. doi: 10.1128/mbio.01468-23.

30 Daw Elbait G, Daou M, Abuoudah M, Elmekawy A, Hasan SW Everett DB, et al. Comparison of qPCR and metagenomic sequencing methods for quantifying antibiotic resistance genes in wastewater. PloS One. 2024 Apr 5;19(4):e0298325. doi: 10.1371/journal.pone.0298325.

31 Knight ME, Webster G, Perry WB, Baldwin A, Rushton L, Pass DA, et al. National-scale antimicrobial resistance surveillance in wastewater: A comparative analysis of HT qPCR and metagenomic approaches. Water Res. 2024 Sep 15;262:121989. doi: 10.1016/j.watres.2024.121989.

32 Taylor W, Bohm K, Dyet K, Weaver L, Pattis I. Comparative analysis of qPCR and metagenomics for detecting antimicrobial resistance in wastewater: a case study. BMC Res Notes. 2025 Jan 8;18(1):5. doi: 10.1186/s13104-024-07027-9.

33 Wang H, Neyvaldt J, Enache L, Sikora P, Mattsson A, Johansson A, et al. Variations among viruses in influent water and effluent water at a wastewater plant over one year as assessed by quantitative

medRxiv preprint doi: https://doi.org/10.64898/2026.08.18.26360688; this version posted August 21, 2026. The copyright holder for this preprint
(which was not certified by peer review) is the author/funder, who has granted medRxiv a license to display the preprint in perpetuity.
It is made available under a CC-BY-NC-ND 4.0 International license .

PCR and metagenomics. Appl Env Microbiol. 2020 Nov 24;86(24):e02073-20. doi: 10.1128/AEM.02073-20.

34 Grimm S, Kaufman J, Rice D et al. Inferring the sensitivity of wastewater metagenomic sequencing for early detection of viruses: a statistical modelling study The Lancet Microbe, 2025; 6

35 Coulliette-Salmond A, Whitehill F, Lyons AK, Abera B, Adler C, Walters MS, Medrzycki M, Ganim C, Campbell M, Lin MY, Poretsky RS, Horton A, Weidhaas J, VanDerslice J, Benson LS, Driver EM, Halden RU, Hamilton KA, Williams M. Healthcare wastewater surveillance: methodological considerations for sampling, feasibility, and implementation. J Water Health. 2026 Jan;24(1):50-64. doi: 10.2166/wh.2025.167. Epub 2025 Dec 22. PMID: 41627796; PMCID: PMC13051650.

36 Sonnenwald, F., Shuttleworth, J., Bailey, O., Williams, M., Frankland, J., Rhead, B., Mark, O., Wade, M. J., & Guymer, I. (2023). Quantifying Mixing in Sewer Networks for Source Localization. *Journal of Environmental Engineering*, *149*(5), 04023019. https://doi.org/10.1061/JOEEDU.EEENG-7134

37 Kohle S, Petersen TN, Vigre H, Johansson MHK, Aarestrup FM (2024) Metagenomic analysis of sewage for surveillance of bacterial pathogens: A release experiment to determine sensitivity. PLoS ONE 19

38 McCall, et al., "Modeling SARS-CoV-2 RNA Degradation in small and large sewersheds" *Environ. Sci. Water Res. and Techno., 8 (*2002)

39 Chow, V. T. (1959). *Open-channel hydraulics*. McGraw-Hill, New York.

40 Massachusetts Department of Environmental Protection. (2023, August 22). 310 CMR 15.00: State Environmental Code, Title 5: standard requirements for the siting, construction, inspection, upgrade and expansion of on-site sewage treatment and disposal systems and for the transport and disposal of septage. https://www.mass.gov/doc/310-cmr-15000-title-5-of-the-state-environmental-code/download

41 Prasek, S.M., et al., Population level SARS-CoV-2 fecal shedding rates determined via wastewater-based epidemiology, Sci. Tot. Env., 838 (2022)

42 Weidhaas, J., et al., Correlation of SARS-CoV-2 RNA in wastewater with COVID-19 disease burden in sewersheds, Sci. Total Environ., 775 (2021)

43 Cummings, J.H., et al., Fecal weight, colon cancer risk, and dietary intake of nonstarch polysaccharides (dietary fiber), Gastroenterology, 103 (1992)

44 Khailany RA, Safdar M, Ozaslan M. Genomic characterization of a novel SARS-CoV-2. Gene Rep. 2020 Jun;19:100682. doi: 10.1016/j.genrep.2020.100682. Epub 2020 Apr 16. PMID: 32300673; PMCID: PMC7161481.

medRxiv preprint doi: https://doi.org/10.64898/2026.08.18.26360688; this version posted August 21, 2026. The copyright holder for this preprint
(which was not certified by peer review) is the author/funder, who has granted medRxiv a license to display the preprint in perpetuity.
It is made available under a CC-BY-NC-ND 4.0 International license .

45 Arts PJ, Kelly JD, Midgley CM, Anglin K, Lu S, et al., 2023. Longitudinal and quantitative fecal shedding dynamics of SARS-CoV-2, pepper mild mottle virus, and crAssphage. mSphere 8:e00132-23.

46 Cummings JH, Bingham SA, Heaton KW, Eastwood MA. Fecal weight, colon cancer risk, and dietary intake of nonstarch polysaccharides (dietary fiber). Gastroenterology. 1992 Dec;103(6):1783-9. doi: 10.1016/0016-5085(92)91435-7. PMID: 1333426.

47 Nanopore Ligation Kit protocol: https://nanoporetech.com/document/ligation-sequencing-gdna-native-barcoding-v14-sqk-nbd114-24?device=PromethION

48 Illumina DNA Prep Reference Guide: https://www.illumina.com/products/by-type/sequencing-kits/library-prep-kits/illumina-dna-prep.html#tabgroup-2-tab1

49 Warish Ahmed et al., Evaluation of process limit of detection and quantification variation of SARS-CoV-2 RT-qPCR and RT-dPCR assays for wastewater surveillance, Water Research, Volume 213, 2022

50 Bushnell, Brian. "BBMap: A Fast, Accurate, Splice-Aware Aligner." (2014).

51 De Coster W, Rademakers R. NanoPack2: population-scale evaluation of long-read sequencing data. Bioinformatics. 2023 May 12;39(5):btad311. doi: 10.1093/bioinformatics/btad311.

52 Wood DE, Lu J, Langmead B. Improved metagenomic analysis with Kraken 2. Genome Biol. 2019 Nov 28;20(1):257. doi: 10.1186/s13059-019-1891-0.

53 Li H. Minimap2: pairwise alignment for nucleotide sequences. Bioinformatics. 2018 Sep 15;34(18):3094-3100. doi: 10.1093/bioinformatics/bty191.

54 Li H, Handsaker B, Wysoker A, Fennell T, Ruan J, Homer N, et al. The sequence alignment/map format and SAMtools. Bioinformatics. 2009 Jun 8;25(16):2078-9. doi: 10.1093/bioinformatics/btp352.

55 Tracey Allen K. Freitas, Po-E Li, Matthew B. Scholz, Patrick S. G. Chain, Accurate read-based metagenome characterization using a hierarchical suite of unique signatures, *Nucleic Acids Research*, Volume 43, Issue 10, 26 May 2015, Page e69, https://doi.org/10.1093/nar/gkv180

56 Interactive Supercomputing on 40,000 Cores for Machine Learning and Data Analysis, Albert Reuther, Jeremy Kepner, Chansup Byun, Siddharth Samsi, William Arcand, David Bestor, Bill Bergeron, Vijay Gadepally, Michael Houle, Matthew Hubbell, Michael Jones, Anna Klein, Lauren Milechin, Julia Mullen, Andrew Prout, Antonio Rosa, Charles Yee, Peter Michaleas, paper presented at the 2018 IEEE High Performance Extreme Computing Conference (HPEC), July 2018.

57 Santos AFB, Nunes M, Filipa-Silva A, Pimentel V, Pingarilho M, Abrantes P, Miranda MNS, Crespo MTB, Abecasis AB, Parreira R, Seabra SG. Wastewater Metavirome Diversity: Exploring Replicate

medRxiv preprint doi: https://doi.org/10.64898/2026.08.18.26360688; this version posted August 21, 2026. The copyright holder for this preprint
(which was not certified by peer review) is the author/funder, who has granted medRxiv a license to display the preprint in perpetuity.
It is made available under a CC-BY-NC-ND 4.0 International license .

Inconsistencies and Bioinformatic Tool Disparities. Int J Environ Res Public Health. 2025 Apr 30;22(5):707

58 Kempf, F., La Ragione, R., Chirullo, B., Schouler, C., & Velge, P. (2022). Super Shedding in Enteric Pathogens: A Review. Microorganisms, 10(11),2101. https://doi.org/10.3390/microorganisms10112101

59 Bejaoui, S., Nielsen, S.H., Rasmussen, A. *et al.* Comparison of Illumina and Oxford Nanopore sequencing data quality for *Clostridioides difficile* genome analysis and their application for epidemiological surveillance. *BMC Genomics* **26**, 92 (2025)

60 Philo SE, De León KB, Noble RT, Zhou NA, Alghafri R, Bar-Or I, Darling A, D'Souza N, Hachimi O, Kaya D, Kim S, Gaardbo Kuhn K, Layton BA, Mansfeldt C, Oceguera B, Radniecki TS, Ram JL, Saunders LP, Shrestha A, Stadler LB, Steele JA, Stevenson BS, Vogel JR, Bibby K, Boehm AB, Halden RU, Delgado Vela J. Wastewater surveillance for bacterial targets: current challenges and future goals. Appl Environ Microbiol. 2024 Jan 24;90(1):e0142823. doi: 10.1128/aem.01428-23. Epub 2023 Dec 15. PMID: 38099657; PMCID: PMC10807411.

61 Davis B, Brown C, Gupta S, Calarco J, Liguori K, Milligan E, et al. Recommendations for the use of metagenomics for routine monitoring of antibiotic resistance in wastewater and impacted aquatic environments. Crit Rev Env Sci Tech. 2023 Mar 01;53(19):1731–1756. doi: 10.1080/10643389.2023.2181620.

62 Yang Y, Deng Y, Liu L, Yin X, Xu X, Wang D, Zhang T. Establishing reference material for the quest towards standardization in environmental microbial metagenomic studies. Water Res. 2023 Oct 15;245:120641. doi: 10.1016/j.watres.2023.120641.

63 Forry SP, Servetas SL, Kralj JG, Soh K, Hadjithomas M, Cano R, et al. Variability and bias in microbiome metagenomic sequencing: an interlaboratory study comparing experimental protocols. Sci Rep. 2024 Apr 29;14(9785). doi: 10.1038/s41598-024-57981-4.

64 Lopez-Labrador FX, Huber M, Sidorov IA, Brown JR, Cuypers L, Laenen L, et al. Multicenter benchmarking of short and long read wet lab protocols for clinical viral metagenomics. J Clin Virol. 2024 Aug;173:105695. doi: 10.1016/j.jcv.2024.105695.